Excitonic correlations in the intermetallic Fe_2VAl

Ruben Weht and W. E. Pickett
Department of Physics, University of California, Davis, California 95616
(Received 12 March 1998)

The intermetallic compound Fe_2VAl looks nonmetallic in transport and strongly metallic in thermodynamic and photoemission data. It has in its band structure a highly differentiated set of valence and conduction bands leading to a semimetallic system with a very low density of carriers. The pseudogap itself is sensitive to the presence of Al states, but the resulting carriers have only minor Al character. The effects of generalized gradient corrections to the local density band structure are shown to be important, reducing the carrier density by a factor of 3. Spin-orbit coupling results in a redistribution of the holes among pockets at the Brillouin zone center. Doping of this nonmagnetic compound by 0.5 electrons per cell in a virtual crystal fashion results in a moment of $0.5\mu_B$ and destroys the pseudogap. We assess the tendencies toward the formation of an excitonic condensate and toward an excitonic Wigner crystal and find both to be unlikely. We propose a model in which the observed properties result from excitonic correlations arising from two interpenetrating lattices of distinctive electrons (e_g on V) and holes (t_{2g} on Fe) of low density (one carrier of each sign per 350 formula units). [S0163-1829(98)03235-4]

I. INTRODUCTION

The electronic behavior of Fe_2VAl has recently been discovered to be highly unusual.[1] The resistivity increases by a factor of 6 from 400 K to 2 K (where $\rho = 3$ mΩ cm), which is characteristic of a nonmetal, but other properties indicate metallic character. A sharp Fermi cutoff is observed in the photoemission spectrum and the specific heat coefficient $\gamma(T) \equiv C/T$ more than doubles below 6 K (to 12 mJ/mol K^2). Ferromagnetism (FM) in the related compounds Fe_3Al and Fe_3Si and probable antiferromagnetism (AF) in Fe_2VSi (Ref. 2) suggest that magnetic behavior may be responsible. The stoichiometric compound itself has no magnetic transition, although the alloy system $Fe_{2+x}V_{1-x}Al$ and the isoelectronic system $Fe_{2+x}V_{1-x}Ga$ (Refs. 3 and 4) are ferromagnetic with a Curie temperature that extrapolates to zero as $x \rightarrow 0^+$. The behaviors of ρ and C/T were suggested[1] as similar to those of heavy fermion metals, which would make it a candidate for a $3d$ based heavy fermion system. If the resistivity peaked and began to decrease below 2 K (as happens for UBe_{13}, for example) the resemblance would be closer; however, the observed value of $\gamma = 12$ mJ/mol K^2 at 2 K is well below that of accepted heavy fermion materials.[5]

Although this compound falls within an alloy system where the V/Fe ratio can be varied continuously, indications are[1] that the properties noted above apply to the material near or at the stoichiometric limit of an ideal Heusler ($L2_1$) structure compound. This structure type is based on an underlying bcc lattice of lattice constant $a/2$, with V at (0,0,0), Al at $(\frac{1}{2},\frac{1}{2},\frac{1}{2})a$, and Fe atoms at $(\frac{1}{4},\frac{1}{4},\frac{1}{4})a$ and $(\frac{3}{4},\frac{3}{4},\frac{3}{4})a$, where $a = 5.761$ Å is the lattice constant of the resulting fcc compound. This structure is also that of Fe_3Al, which has two inequivalent Fe sites. The Fe_I site (which is the V site in Fe_2VAl) has eight Fe neighbors in an octahedral configuration, while the Fe_{II} site has four Fe and four Al neighbors. In $Fe_{2+x}V_{1-x}Al$ the larger V atoms occupy the Fe_I site for $x \leqslant 0$. This trend is followed by all transition metal atoms to the left of Fe in the Periodic Table (Ti, V, and Cr).[6]

Guo, Botton, and Nishino[7] and Singh and Mazin[8] have reported local density functional results that indicate that Fe_2VAl is a low carrier density, compensated semimetal. Γ-centered holes of Fe t_{2g} antibonding character are compensated by zone-edge X-point holes of V e_g character. Because the data cannot be interpreted simply in terms of degenerate, noninteracting carriers with this semimetallic band structure, Singh and Mazin suggest that the behavior is caused by strong spin fluctuations of Fe atoms on the V site, due to nonstoichiometry or to antisite defects.

In this paper we discuss other possible causes of the peculiar observed behavior, starting from the semimetallic band structure obtained in the local density approximation (LD). We show that Al plays a crucial, but ultimately indirect, part in determining the electronic structure and that the magnetic state is unusually sensitive to band filling. Based on a calculated carrier density of one electron and one hole for each 350 unit cells, we consider parameters related to a possible excitonic condensate or to an excitonic Wigner crystal. These exotic phases are not favored by the parameters. The character and density of the carriers, the structure of their sublattices, and the anticipated dielectric behavior suggest that dynamic correlations of excitonic character are candidates to account for the enhanced ''metallic'' spectral density that is accompanied by decreasing conduction.

II. METHOD OF CALCULATION

We have used the linearized augmented plane wave (LAPW) method[9] that utilizes a fully general shape of density and potential. Both the WIEN97 code[10] and the WM-NRL code[11] have been used on different aspects of the calculations. The lattice constant of 5.761 Å was used. LAPW sphere radii (R) of 2.00–2.30 a.u. were used in various calculations, and with very well converged basis sets no discernible effect of sphere radius size was found. Cutoffs of RK_{max} up to 8.6–8.9 provided well converged basis sets varying from 330 to more than 500 functions per primitive

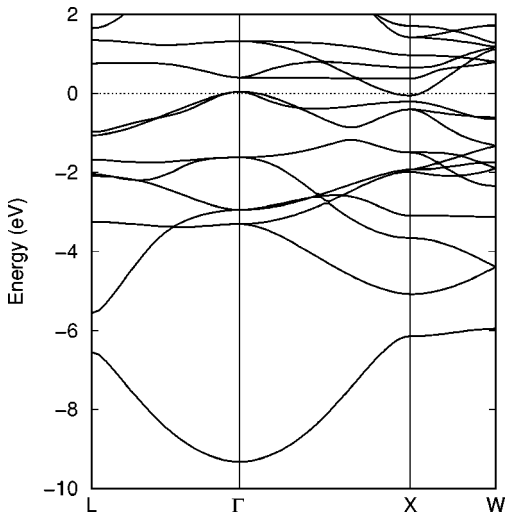

FIG. 1. Full band structure of Fe_2VAl along principle symmetry lines. The dashed line denotes the Fermi level. The lower band is *s*-like, primarily Al character. The Fe and V *d* bands lie between −5 and 2 eV.

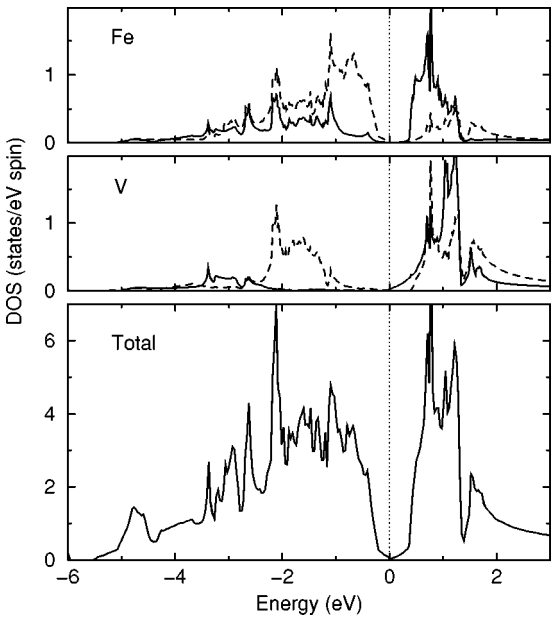

FIG. 2. Density of states of Fe_2VAl (bottom panel), projected onto the e_g (solid lines) and t_{2g} (dashed lines) crystal field characters of the Fe (top panel) and V (middle panel) atoms. Note that the Fermi level falls precisely in the minimum, which is shown in more detail in Fig. 5.

cell. Self-consistency was carried out on *k*-point meshes of around 200 points in the irreducible Brillouin zone ($12\times12\times12$ and $15\times15\times15$ meshes).

To assess the finer details of the predictions of density functional theory, we used two forms of generalized gradient corrected exchange-correlation functionals from Perdew and co-workers.[12] Gradient corrected functionals have been observed to give small but sometimes important corrections to the band structure in several compounds. Spin-orbit coupling was included in a second variation approach as formulated by MacDonald *et al.*[13]

III. CALCULATIONAL RESULTS

A. LDA band structure

The band structure of Fe_2VAl is shown in Fig. 1. The crucial feature is a disjointedness between occupied valence bands and unoccupied conduction bands that is unusual in an intermetallic compound. There are 12 bands to be filled by the valence electrons. Interestingly, these lower 12 bands are disconnected from the remaining bands throughout the Brillouin zone. The result is not quite a gap but rather a deep minimum (pseudogap) in the density of states (DOS) precisely where the Fermi level (E_F) falls. The density of states $N(E_F)$ does not vanish because there is a very small overlap of a V-derived conduction band minimum, containing electron carriers at the three inequivalent *X* points, with a threefold degenerate $\Gamma_{25'}$ valence band maximum arising from Fe-derived holes.

The hole band at Γ is roughly 40% t_{2g} on each Fe atom and 15% V, with minor Al character. The electron pockets at *X* are V e_g states (with minor Al character), but Fe *d* character is forbidden by symmetry. The total and atom decomposed and projected DOS's are shown in Fig. 2. The Al states (not shown here, but presented by Guo *et al.*[7]) are repelled from a wide region including the Fermi level by the strong *d*-*d* bonding, as discussed by Singh and Mazin. This repulsion, as well as the apparent unimportance of the Al atom, leaves a network that can be pictured as V-centered cubic VFe_8 clusters connected along all edges in a fcc arrangement.

Contour plots of the holes and the electrons in a (110) plane that contains the nearest neighbor separations are shown in Fig. 3. The t_{2g} character of the holes is not so apparent in this plane, but they show the normal d_{xy} shape when plotted in the (001) plane. It is apparent from Fig. 3 that the hole and electron wave functions are essentially nonbonding and this character impacts the model we present in Sec. IV.

The DOS shown in Fig. 2 is projected onto e_g and t_{2g} states on both Fe and V. The Fe t_{2g} states lie almost entirely below E_F, whereas the Fe e_g DOS is split into roughly equal amounts below and above the pseudogap. For V the e_g states

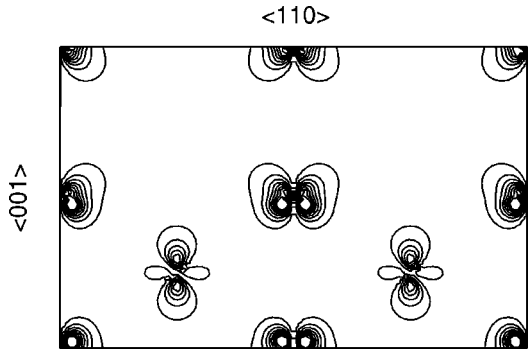

FIG. 3. Contour plot of the Fe-centered hole carriers (from the Γ point valence band maximum) and the *e*-*g*–type V-centered electron carriers (from the *X* point minimum) in Fe_2VAl, plotted in the (110) plane. Al atoms are centered in the empty regions. The separate densities were added to produce this figure. The t_{2g}-type density on Fe (corners, edges, and center of the plot) looks normal when viewed in a (100) plane, as is normally done.

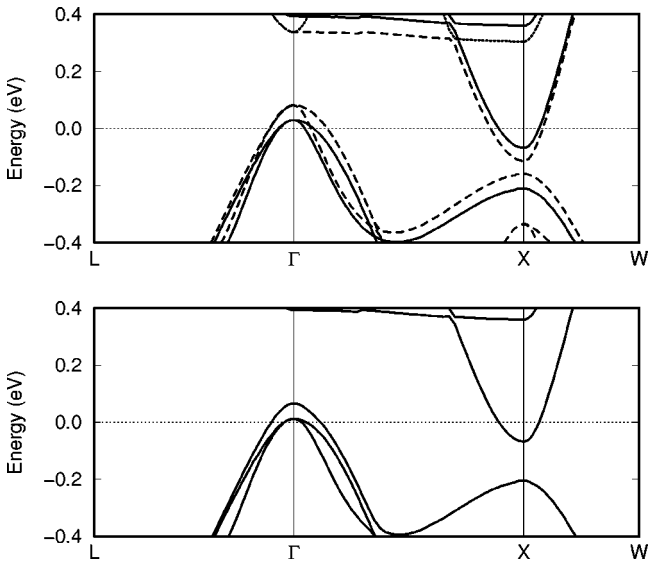

FIG. 4. Enlargement of the band structure of Fe_2VAl near the Fermi level. The upper panel shows how gradient corrections affect the band overlap (dashed lines show bands before gradient corrections are included) by shifting states at X. Both gradient corrections and spin-orbit coupling are included in the lower panel.

lie entirely above the pseudogap, while the t_{2g} states form bonding-antibonding complexes separated across the gap by 3 eV.

The minimum direct gap of approximately 0.2 eV occurs along the (100) directions near X. A ''Penn gap'' between the occupied and unoccupied DOS's, which gives a rough measure of where there is substantial absorption weight, would be at least 2 eV. The susceptibility of this system is discussed below.

B. Gradient corrections and spin-orbit coupling

1. Gradient corrections

The LDA band structure we obtain without gradient corrections and neglecting spin-orbit coupling is indistinguishable from that of previous work.[7,8] Since the fine details are of interest in determining the predicted effective masses and carrier densities, we have calculated the generalized gradient corrections of Perdew and co-workers[12] and also included spin-orbit coupling.[13] The resulting bands are those shown in Fig. 1 and an enlargement near the Fermi level is pictured in Fig. 4. Gradient corrections lead to a shift of the X point conduction minimum upward with respect to the Γ point band maximum, by 95 meV. This reduces the band overlap (before spin-orbit coupling) from 200 meV to 100 meV and reduces the number of carriers by roughly $(100/200)^{3/2} \approx \frac{1}{3}$.

2. Spin-orbit coupling

The result of spin-orbit coupling is to split the triply degenerate $\Gamma_{25'}$ band maximum of mostly Fe t_{2g} character into $j=\frac{3}{2}$ and $j=\frac{5}{2}$ levels separated by 56 meV. The lower doublet leads to a pair of hole pockets whose occupation is an order of magnitude less than that of the remaining hole pocket. The result is that the number of hole carriers is affected only a little, but the ''degeneracy'' is lifted and the Fermi wave vector of the holes is increased by $3^{1/3} \approx 1.4$.

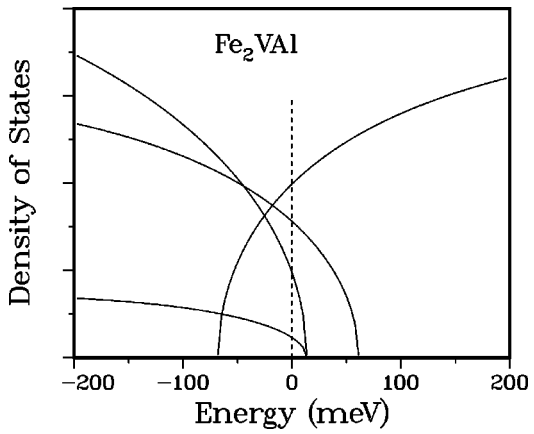

FIG. 5. Relative densities of states of the overlapping bands very near the Fermi level, from a small wave vector expansion discussed in the text. Two of the hole bands are nearly unoccupied and are neglected in the discussion in the text.

3. Determination of the Fermi level

To determine the position of the Fermi level, the hole pocket and the electron ellipsoids at X were fit along high symmetry directions to small wave vector expansions

$$\varepsilon_k = \varepsilon_0 + \alpha k^2 + \beta k^4. \tag{1}$$

Since the k^4 term is important even though the Fermi energy is small, effective masses do not describe the dispersion precisely. We obtain roughly $m_h^* \approx 1.0-1.1$ m for the main hole pocket and $m_{\ell}^* = 0.8m$ and $m_{tr}^* = 0.3-0.35$ m for the longitudinal and transverse electron masses at X. The band overlap is 130 meV and compensation determines the Fermi levels of 70 meV for the large hole pocket and 60 meV for electrons (relative to their respective band edges). The DOS's of the various pockets are shown in Fig. 5.

We finally obtain $N(E_F) \approx 0.1$ states/eV, corresponding to a bare band specific heat coefficient $\gamma_b \approx 0.2$ mJ/mol K^2. Compared to the extrapolated $(T \to 0)$ observed value[1] of 14 mJ/mol K^2, the apparent enhancement factor of the thermal mass is $m_{th}/m_b \approx 70$. We address this discrepancy in Sec. IV.

4. Mechanical properties and effect of pressure

We calculated the energy for several crystal volumes a few percent on either side of the experimental volume. The lattice constant that minimizes the energy is 0.7% smaller than the experimental value $(V/V_{obs} = 0.98)$. A fit to a polynomial gives a bulk modulus $B = 0.49$ Mbar. This indicates a relatively soft lattice, which can be compared to 1.7 Mbar for Fe and 0.7 Mbar for Al.

It will be of interest for future experiments what the effect of pressure on the band overlap of the semimetallic state is. From calculations at $V = 1.025V_{obs}$ and $V = 0.95V_{obs}$, which translates to a pressure difference of 36 kbar, the change in band overlap is negligible. Hence we predict that the effect of even substantial pressure on the semimetallic state will be small.

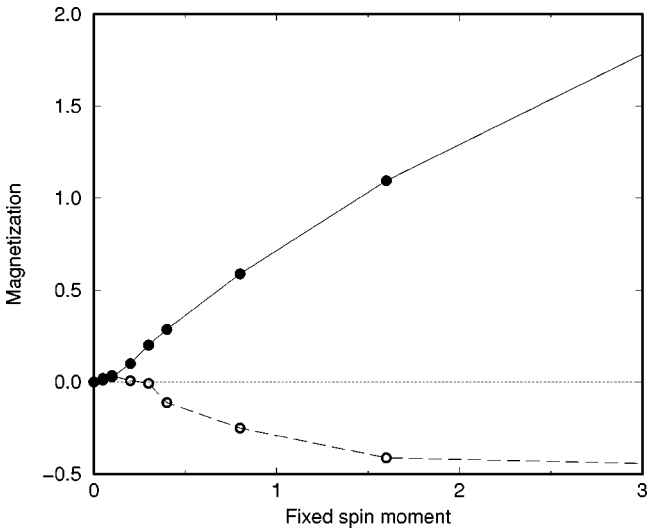

FIG. 6. Behavior of the moments on the Fe atom (solid dots) and on the V atom (open dots) when fixed spin moment calculations are carried out. Calculations were actually carried out for moments above $3\mu_B$ as well as for the points indicated.

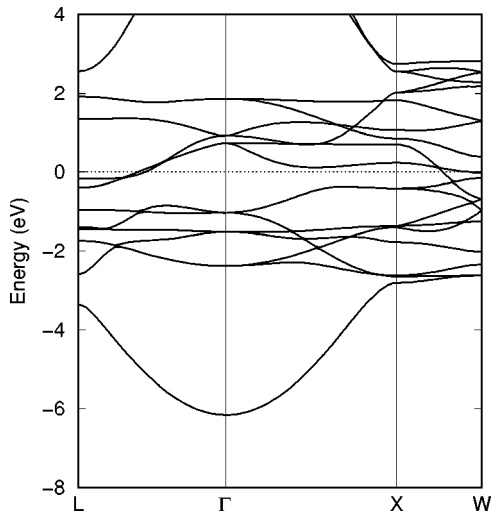

FIG. 7. Band structure of the fictition compound Fe_2V, after the removal of the Al atom. The d bands narrow by at least 1.5 eV and the band topology near the Fermi level rearranges.

C. Magnetic tendencies of Fe_2VAl

We have checked for a ferromagnetic instability by performing fixed spin moment calculations. No such instability was found, consistent with the results of Singh and Mazin and also with expectations based on the very small value of $N(E_F)$, which would leave the system far from a Stoner instability. For small forced moments the V moment is parallel to that on the Fe ion and the energy vs moment curve is parabolic. For total moment greater than $0.3\mu_B$, however, the V moment becomes antiparallel and saturates around $0.5\mu_B$ as the Fe moments are driven to $2\mu_B$ and above. This behavior is plotted in Fig. 6. In this range the energy vs moment curve is linear.

A FM instability involves the $\vec{q}=0$ response of the system, which is weak due to the very small Fermi surfaces. The band structure contains a more interesting low energy response at the zone boundary (X point) wave vector $\vec{Q}_{100}=(1,0,0)2\pi/a$, which could encourage an AF instability. This response arises from the intersection of the Fermi surfaces when the hole-derived surfaces at Γ are displaced by $\vec{Q}_{100}$. We searched for AF ordering of the simple cubic Fe sublattice, with cubic (rocksalt) ordering of Fe moments. The energy increases monotonically with the Fe moment (arising from the imposed external staggered field H_{st}) and no tendency toward instability was found. These results are consistent with the lack of any observed magnetic order.

D. Characteristics of the semimetallic state

The predicted carrier concentration is 2.9×10^{-3} carriers of each sign per formula unit (or one per $350\approx 7\times7\times7$ primitive cells). This number is four times smaller than that reported by Singh and Mazin due to the effect of the generalized gradient corrections to LDA, which push the electron band at X upward and thereby acts to decrease the band overlap and hence the carrier concentration. Since the electron carriers are V e_g character, they reside on the V sites that form a fcc lattice. The hole carriers are of primarily Fe t_{2g} character and the Fe sites form a sc array of lattice constant $a/2$, on which the holes are an average of $(350)^{1/3}(a/2)\approx20$ Å apart.

For qualitative purposes we can think in terms of a mass $m_h^*\approx1$ for holes with 1/700 of sites occupied and mass $m_e^*\approx0.5$ of electrons with 1/350 of available sites occupied. Taking the Drude plasma frequencies as $\Omega_p=4\pi ne^2/m^*$ gives $\hbar\Omega_p=70$ meV for the holes and 50 meV for the electrons.

E. Importance of the Al site

Singh and Mazin[8] have noted that the Al sp orbitals mix with the transition metal d states, with the result that little of the Al DOS remains in the vicinity of the Fermi level. Since isoelectronic Fe_2VGa has properties[3,4] similar to those of Fe_2VAl, we have carried out parallel calculations on the Ga compound at its lattice constant of 5.776 Å.[3,4] The resulting band structure is very similar. The (primarily Ga) s band centered 9.3 eV below E_F is 1 eV lower than the Al band in Fe_2VAl, but other differences are smaller. The band overlap giving rise to semimetallic character is 230 meV, compared to 130 meV in the Al compound. As a result, Fermi surface sizes and carrier concentrations are correspondingly larger than in Fe_2VAl.

To explore further the effect of the Al states, we calculated the band structure of the fictitious compound Fe_2V in which the Al atom is simply removed. Since this unit cell has an odd number of electrons, the electronic structure must differ qualitatively; it cannot be a paramagnetic semiconductor or be isomorphic to one (as the Fe_2VAl band structure is). The resulting band structure is shown in Fig. 7. The difference in the electronic structure is substantial and is most obvious along the X-W direction.

The combined Fe-V d bands are considerably narrower, but corresponding bands can be located throughout the Brillouin zone and throughout the valence/conduction band energy range. This congruity of the band structures indicates that removal of Al is analogous to removing three valence electrons from the cell without removing bands (basis states

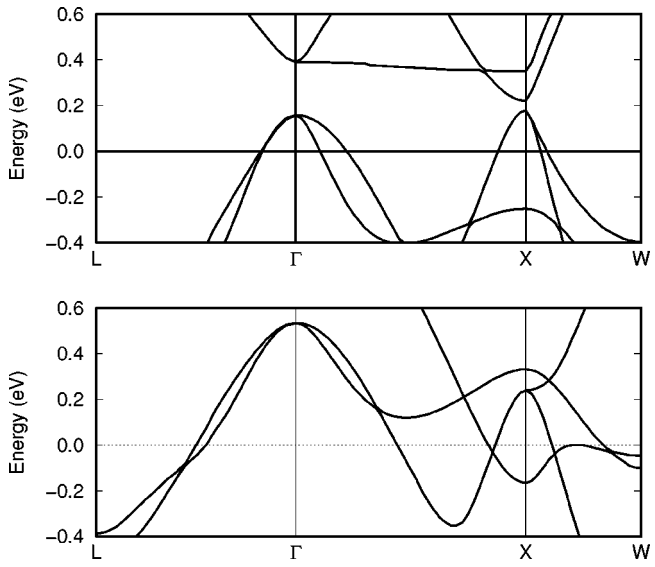

FIG. 8. (a) Majority and (b) minority band structures of the ferromagnetic state of the virtual crystal of $Fe_2V_{1/2}Cr_{1/2}Al$, illustrating the strong deviation from a simple Stoner splitting of the bands in this system.

available for occupation). As a result, there is $d \rightarrow s$ charge promotion on both Fe and V as the lowest, primarily s-like, band changes from largely Al character to totally Fe and V character. The filling of the d bands drops, with an entire band along Γ-X-L becoming unoccupied and two bands along Γ-L becoming half empty. Relative band shifts are also substantial and the resulting change in band topology leads to the complete disappearance of the pseudogap due to band rearrangements at the W point. Thus the Al atom or at least its three electrons play a crucial role in determining the electronic behavior of Fe_2VAl. The active states at the Fermi level nevertheless have only a small amount of Al character, as emphasized by Singh and Mazin.[8]

F. Doping on the V sublattice

As an indication of the effect of replacing V with a heavier transition metal atom, a virtual crystal calculation was carried out for the case where the charge on the V nucleus and the number of electrons are increased by 0.5. This corresponds roughly to the case of $Fe_2V_{1/2}Cr_{1/2}Al$, or more roughly to $Fe_2V_{5/6}Fe_{1/6}Al$. The result is a ferrimagnetic state with a net moment near $0.5\mu_B$, i.e., almost equal to the extra electronic charge in the cell. The band structure, shown in Fig. 8 in a region near the Fermi level, is severely disrupted near E_F, not resembling at all a situation in which the bands are rigidly split in a Stoner fashion. The convergence to a self-consistent solution was very slow, suggesting that the FM state should not be very stable. The net moment is derived from $0.52\mu_B$ within each Fe sphere and $-0.45\mu_B$ within the V sphere.

We have looked at the same doping level by doing a virtual calculation using the Al site, i.e., treating $Fe_2VAl_{1/2}Si_{1/2}$. Considering the behavior we found in Sec. III E, that Al seems to simply dump its electrons into the system, this virtual crystal calculation may be a very realistic treatment of the Al-Si alloy. The result is very similar to doping on the V sublattice: The ferrimagnetic moment is again near $0.5\mu_B$, with 0.42 on each Fe atom and -0.26 on each V atom. The differences between doping on the V and Al sublattices can be accounted for almost entirely by the lowering of the V-derived electron bands when doping is done on the V site. We will report more of these results and a study of Fe_2VSi elsewhere.

IV. DISCUSSION OF EFFECTS OF INTERACTIONS

A. Excitonic condensate?

The study of semiconducting or semimetallic systems in which the gap E_g (positive or negative) is very small has a long history, with residual interactions leading to the possibility of several exotic phases. A spontaneous condensed exciton phase is possible[14] when the gap E_g is less than the exciton binding energy E_B^x. The occurrence of the spontaneous excitonic phase in a narrow gap semiconductor or low density semimetal has been extensively studied and searched for experimentally, but only a few systems such as $TmSe_{0.45}Te_{0.55}$ provide reasonable candidates for such a system.[15] Specific theoretical predictions are quite sensitive to the size and shape of the electron and hole Fermi surfaces.[16] The possibility of an exciton condensate in more highly correlated systems such as Kondo insulators has been suggested by Duan, Arovas, and Sham.[17]

The classic case of the group V semimetals lies at one extreme, where a one-electron picture works well and the effect of residual interactions is small. Bismuth is a compensated semimetal with less than 10^{-5} electron and hole carriers per atom, yet it behaves at low temperature as a straightforward degenerate metal with observable (but tiny) Fermi surfaces. An intermediate case is represented by ScN, a rock-salt structure semimetal with a LDA band structure very much like that of Fe_2VAl: a calculated band overlap of 80 meV involving a threefold degenerate Γ_{15} hole pocket at Γ and electron ellipsoids at X. Monnier *et al.*[18] considered the additional correlation energy of the electron and hole carriers within the LDA and concluded that ScN remains semimetallic (i.e., an electron-hole liquid) with only modestly renormalized band overlap and effective masses.

The present case of Fe_2VAl has two features not included in previous models.[14,16] First, the electrons and holes are well confined to distinct interpenetrating lattices so that the discreteness of the lattice may have an effect. Second, there are likely to be strong residual interactions. There will be repulsive electron-electron and hole-hole interactions, not only on-site but also intersite due to the weakness of the metallic screening. On-site exchange interactions on Fe and V may lead to magnetic fluctuations, although they should be much suppressed due to the low value of $N(E_F)$. Then there will be the attractive electron-hole interactions.

The response is described by the dielectric function $\varepsilon = 1 - \hat{v}\chi_0$ where $\hat{v}$ is a mean matrix element of the Coulomb interaction and the noninteracting susceptibility is

$$\chi_0(\vec{q},\omega) = 2\sum_{k,n,m} \frac{f(\varepsilon_{k,n}) - f(\varepsilon_{k+q,m})}{\varepsilon_{k+q,m} - \varepsilon_{k,n} - \hbar\omega}, \tag{2}$$

where $\varepsilon_{k,n}$ is the band energy of band n and $f(\varepsilon)$ is the Fermi-Dirac thermal occupation factor. For the band struc-

ture of Fe_2VAl there are three types of contributions at low energy $\hbar\omega$. For $\vec{q}\to 0$ there is the usual repulsive intraband scattering (from holes and electrons separately) that gives rise to Drude absorption in the optical spectrum. This response corresponds to a Lindhard-like susceptibility from both the hole and electron pockets, with Drude plasma energies given in Sec. III D. The characteristic Fermi wavelengths are of the order of $\lambda_F \approx 12a = 70$ Å.

Second, near the X point where $\vec{q}=\vec{Q}_{100}$ and equivalent points there will be low ω response as the Γ-centered hole Fermi surface displaced by $\vec{Q}_{100}$ intersects one of the electron ellipsoid Fermi surfaces. Third, there will be low energy intervalley scattering of electrons centered at $\vec{Q}_{110} = (1,0,0)(2\pi/a) - (0,-1,0)(2\pi/a)$ and symmetry-related vectors. In the fcc lattice $\vec{Q}_{110}$ reduces to $\vec{Q}_{100}$. Thus attractive electron-hole scattering and intervalley repulsive electron-electron scattering occur at the same reduced wave vectors.

B. Excitonic parameters

The scale factors describing the excitonic system[18] depend on the background dielectric constant ϵ_∞ for the rigid lattice in the absence of carriers and on the reduced mass μ given by

$$\frac{1}{\mu} = \frac{1}{m_e^*} + \frac{1}{m_h^*}, \tag{3}$$

where the electron effective mass m_e^* is given by

$$\frac{3}{m_e^*} = \frac{1}{m_{/\!/}} + \frac{2}{m_{tr}} \tag{4}$$

in terms of the longitudinal ($m_{/\!/}$) and transverse (m_{tr}) masses of the electron ellipsoid. For the calculated bands we obtain $\mu \approx \frac{1}{3}m$. The density of electron-hole pairs corresponds to a (bare; see below) density parameter $r_s = 30$. The dielectric constant is difficult to estimate. It involves dipole matrix elements between d bands, which vanish in the atomic limit (dipole transitions require $p\to d$ or $d\to f$ transitions in this limit). Moreover, the valence and conduction bands are dominated by Fe and V, respectively, on two separate sublattices, which will tend to reduce matrix elements. Since the Fe and V d states retain much of their atomic character in this solid, we do not expect a large value of ϵ_∞.

The exciton radius a_B^x, effective Rydberg E_B^x (the binding energy), and density parameter r_s^x are given by[18]

$$a_B^x = \epsilon_\infty \frac{m}{\mu} a_B, \tag{5}$$

$$E_B^x = \frac{1}{\epsilon_\infty^2}\frac{\mu}{m} E_R, \tag{6}$$

and

$$r_s^x = \frac{a_B}{a_B^x} r_s = \frac{1}{\epsilon_\infty}\frac{\mu}{m} r_s, \tag{7}$$

TABLE I. Values of the excitonic radius a_B^x, binding energy E_B^x, and density parameter r_x^x for representative values of ϵ_∞.

ϵ_∞	a_B^x/a_B	E_B^x (meV)	r_s^x
2	6	1150	5
5	15	180	2
10	30	45	1
20	60	11	0.5

where E_R is the Rydberg and a_B is the Bohr radius. In Table I we provide values of these parameters for $\epsilon_\infty = 2$, 5, 10, and 20. From the band structure and the band character we expect ϵ_∞ to lie in the lower end of this range. In any case, however, the exciton radius is large and the resulting effective density parameter r_s^x is far from the low density range where an exciton condensate might be expected. Moreover, the Thomas-Fermi screening length for this density of electrons (or holes) is still approximately equal to 2 Å, so screening is still a consideration. In any case, a true exciton condensate would be an insulator, which is not the case for the reported samples (unless the conduction is a result of defects). Thus an exciton condensate is not expected to arise. Moreover, since there is only a factor of 2 difference in masses, a hole Wigner crystal screened by the lighter electrons also is not a likely scenario. However, an electron-hole plasma of low density ($r_s = 30$) may have strong dynamic correlations, which we address next.

C. Excitonic correlations

An interaction that will be nearly unscreened in this system is the attraction between an electron on a V site and a hole on a neighboring Fe site. The V-Fe separation is only 2.5 Å, and since the density of electrons and holes separately is in the vicinity (if ϵ_∞ is small) of that where Wigner crystallization should occur,[19] a homogeneous screening approximation may have broken down anyway. We suggest that a Hamiltonian of the form

$$\begin{aligned} H = &\sum_{i,i',s} t^e_{i,i'} e^\dagger_{i,s} e_{i',s} + \sum_{j,j',s} t^h_{j,j'} h^\dagger_{j,s} h_{j',s} \\ &- V^{eh} \sum_{\langle i,j\rangle,s,s'} n^e_{i,s} n^h_{j,s'} + U^e \sum_i n^e_{i,+} n^e_{i,-} \\ &+ U^h \sum_j n^h_{j,+} n^h_{j,-} \end{aligned} \tag{8}$$

includes the important residual interactions. Here $e^\dagger_{i,s}$ creates an electron of spin s (equal to $+$ or $-$) on the ith site of the V sublattice, $h^\dagger_{j,s}$ creates a hole of spin s on the jth site of the Fe sublattice, $n^e = e^\dagger e$, and similarly for the hole occupation operator. The constants V^{eh} and U^e, U^h represent the corresponding interactions confined here to on-site for like particles or nearest neighbors for the electron-hole interaction. The hopping amplitudes t^e and t^h are determined so as to reproduce the dispersion seen in Fig. 4. The attractive e-h attraction V^{eh} might be of the order of

$$V^{eh} \geqslant \frac{e^2}{\epsilon_\infty r_{NN}} e^{-k_{TF} r_{NN}} = \frac{2.5\ \text{eV}}{\epsilon_\infty} \times 0.3 \approx 150\ \text{meV} \tag{9}$$

if $\epsilon_\infty \approx 5$, with the equality being applicable only if Thomas-Fermi screening is applicable. If both dielectric and Thomas-Fermi screening are inapplicable due to the short separation, V^{eh} could approach the 1–2 eV range.

Falicov and Kimball[20] considered such a model, but treated only the case of infinitely heavy holes and neglect of identical particle repulsion. They obtained an anomalous temperature dependence of the carrier concentration. Kasuya[21] has considered the possibility of Wigner crystallization of excitons in a related picture and suggested that that picture might be appropriate for rare earth pnictides such as LaSb. The situation presented by Fe_2VAl does not seem to fit well within either of these pictures.

Since we expect the kinetic energy to be sufficient to inhibit the formation of bound excitons (as discussed in Sec. IV B), dynamic correlations of excitonic character may be substantial. To account for the observed behavior, the interactions have to be large enough to keep the system from simply reverting to a degenerate metal (such as Bi). Two effects oppose the formation of coherent propagating electron-hole pairs: The electrons and holes have different velocities (although very similar in magnitude) and they move on inequivalent sublattices. Nevertheless, excitonic correlations should occur and grow in strength as the temperature is lowered. These correlations result in neutral objects that do not carry current, hence the resistivity should increase at low temperature, as observed, as carriers are effectively removed in pairs from the conduction process. Whether the photoemission spectra and the thermal mass enhancement can be obtained will require further treatment of this model Hamiltonian, which will be presented elsewhere. This Hamiltonian would be expected to show superconductivity in its phase diagram as well, although perhaps not at very low density.

V. SUMMARY

Within the local density approximation, Fe_2VAl is found to be a low density semimetal. It is not unstable toward magnetic ordering, in agreement with observation, although the addition of rather small amounts of carriers produces ferromagnetism, as observed. The Al atom is found to have a strong but indirect effect on the electronic structure of this compound. The observed properties, including a heat capacity that is 70 times larger than the semimetallic DOS can account for, indicate that other processes are occurring in this system.

The density of electrons and holes is in the range where individual formation of a Wigner crystal is expected and hence long-range interactions might be expected to be of importance. We have suggested rather that dynamic exciton-like short-range correlations (arising from short-range interactions) will dominate the observed behavior and account for at least some of the enhancement of the thermal mass and for the upturn in the resistivity at low temperature. We have considered the possibility of an exciton condensate ground state, but for this picture to be viable even for an unreasonably small background dielectric constant, a conventional condensate does not seem to be indicated. A two-band, extended Hubbard model with attractive electron-hole interaction has been suggested as a possible model to capture the essential processes, including excitonic correlations. The possibility of inhomogeneous magnetism, as suggested by Singh and Mazin, remains a possibility for accounting for some of the observed behavior.

ACKNOWLEDGMENTS

We are grateful to W. L. Lambrecht for bringing Ref. 18 to our attention. This work was supported by the U. S. Office of Naval Research Grant No. N00014-97-1-0956.

[1] Y. Nishino, M. Kato, S. Asano, K. Soda, M. Hayasaki, and U. Mizutani, Phys. Rev. Lett. **79**, 1909 (1997).
[2] K. Endo, H. Matsuda, K. Ooiwa, and K. Itoh, J. Phys. Soc. Jpn. **64**, 2329 (1995).
[3] K. Endo, H. Matsuda, K. Ooiwa, M. Iijima, K. Ito, T. Goto, and A. Ono, J. Phys. Soc. Jpn. **66**, 1257 (1997).
[4] N. Kawamiya, Y. Nishino, M. Matsuo, and S. Asano, Phys. Rev. B **44**, 12 406 (1991).
[5] G. R. Stewart, Rev. Mod. Phys. **59**, 755 (1984).
[6] D. E. Okpalugo, J. G. Booth, and C. A. Faunce, J. Phys. F **15**, 681 (1985).
[7] G. Y. Guo, G. A. Botton, and Y. Nishino, J. Phys.: Condens. Matter **10**, L119 (1998).
[8] D. J. Singh and I. I. Mazin, Phys. Rev. B **57**, 14 352 (1998).
[9] D. J. Singh, *Planewaves, Pseudopotentials, and the LAPW Method* (Kluwer Academic, Boston, 1994).
[10] P. Blaha, K. Schwarz, and J. Luitz, WIEN97, Vienna University of Technology, 1997. This is an improved and updated version of the original copyrighted WIEN code, which was published by P. Blaha, K. Schwarz, P. Sorantin, and S. B. Trickey, Comput. Phys. Commun. **59**, 399 (1990).
[11] S. H. Wei and H. Krakauer, Phys. Rev. Lett. **55**, 1200 (1985); D. J. Singh, Phys. Rev. B **43**, 6388 (1991).
[12] J. P. Perdew, J. A. Chevary, S. H. Vosko, K. A. Jackson, M. R. Pederson, D. J. Singh, and C. Fiolhais, Phys. Rev. B **46**, 6671 (1992); J. P. Perdew, K. Burke, and M. Ernzerhof, Phys. Rev. Lett. **77**, 3865 (1996).
[13] A. H. MacDonald, W. E. Pickett, and D. D. Koelling, J. Phys. C **13**, 2675 (1980).
[14] B. I. Halperin and T. M. Rice, Rev. Mod. Phys. **40**, 756 (1968).
[15] B. Bucher, P. Steiner, and P. Wachter, Phys. Rev. Lett. **67**, 2717 (1991).
[16] Yu. V. Kopaev and T. T. Mnatsakanov, Fiz. Tverd. Tela **15**, 744 (1973) [Sov. Phys. Solid State **15**, 520 (1973)].
[17] J.-M. Duan, D. P. Arovas, and L. J. Sham, Phys. Rev. Lett. **79**, 2097 (1997).
[18] R. Monnier, J. Rhyner, T. M. Rice, and D. D. Koelling, Phys. Rev. B **31**, 5554 (1985).
[19] H. B. Shore, E. Zaremba, J. H. Rose, and L. Sander, Phys. Rev. B **18**, 6506 (1978), find crystallization to occur around $r_s = 26$.
[20] L. M. Falicov and J. C. Kimball, Phys. Rev. Lett. **22**, 997 (1969).
[21] T. Kasuya, J. Phys. Soc. Jpn. **61**, 2206 (1992).